Am. J. Hum. Genet. 63:1411–1418, 1998

Autosomal Dominant Nanophthalmos (*NNO1*) with High Hyperopia and Angle-Closure Glaucoma Maps to Chromosome 11

M. I. Othman,[1] S. A. Sullivan,[4] G. L. Skuta,[4] D. A. Cockrell,[5] H. M. Stringham,[2] C. A. Downs,[1] A. Fornés,[1] A. Mick,[1] M. Boehnke,[2] D. Vollrath,[6] and J. E. Richards[1,3]

Departments of [1]Ophthalmology, [2]Biostatistics, and [3]Epidemiology, University of Michigan, Ann Arbor; [4]Dean A. McGee Eye Institute, Department of Ophthalmology, University of Oklahoma, Oklahoma City; [5]Cockrell Eye Care Center, Inc., Stillwater, OK; [6]Department of Genetics, Stanford University, Stanford, CA

Summary

Nanophthalmos is an uncommon developmental ocular disorder characterized by a small eye, as indicated by short axial length, high hyperopia (severe farsightedness), high lens/eye volume ratio, and a high incidence of angle-closure glaucoma. We performed clinical and genetic evaluations of members of a large family in which nanophthalmos is transmitted in an autosomal dominant manner. Ocular examinations of 22 affected family members revealed high hyperopia (range +7.25–+13.00 diopters; mean +9.88 diopters) and short axial length (range 17.55–19.28 mm; mean 18.13 mm). Twelve affected family members had angle-closure glaucoma or occludable anterior-chamber angles. Linkage analysis of a genome scan demonstrated highly significant evidence that nanophthalmos in this family is the result of a defect in a previously unidentified locus (*NNO1*) on chromosome 11. The gene was localized to a 14.7-cM interval between D11S905 and D11S987, with a maximum LOD score of 5.92 at a recombination fraction of .00 for marker D11S903 and a multipoint maximum LOD score of 6.31 for marker D11S1313. *NNO1* is the first human locus associated with nanophthalmos or with an angle-closure glaucoma phenotype, and the identification of the *NNO1* locus is the first step toward the cloning of the gene. A cloned copy of the gene will enable examination of the relationship, if any, between nanophthalmos and less severe forms of hyperopia and between nanophthalmos and other conditions in which angle-closure glaucoma is a feature.

Received June 25, 1998; accepted for publication September 14, 1998; electronically published October 30, 1998.

Address for correspondence and reprints: Julia E. Richards, W. K. Kellogg Eye Center, 1000 Wall Street, Ann Arbor, MI 48105; E-mail: richj@umich.edu. Or, Gregory L. Skuta, Dean A. McGee Eye Institute, University of Oklahoma Health Science Center, 608 Stanton L. Young Boulevard, Oklahoma City, OK 73104; E-mail: gregory-skuta@ouhsc.edu

0002-9297/98/6305-0018$02.00

Introduction

Nanophthalmos, sometimes referred to as "simple (or pure) microphthalmos" (Brockhurst 1974; Weiss et al. 1989; Vingolo et al. 1994), is a relatively rare condition characterized by a small eye (globe) in the absence of any systemic abnormalities. Both autosomal recessive and autosomal dominant inheritance have been reported for nanophthalmos (Martorina 1988; Diehl et al. 1989; Vingolo et al. 1994). The major clinical characteristics of the nanophthalmic eye include a short axial length, a high degree of hyperopia (farsightedness), a high lens/eye volume ratio, a small corneal diameter, and a high occurrence of angle-closure glaucoma (Duke-Elder 1964; Kimbrough et al. 1979; Singh et al. 1982).

Nanophthalmos can result in severe visual consequences. Nanophthalmic individuals are farsighted because the shortened axial length causes the focal point to fall behind the retina, a condition that can be treated with appropriate corrective lenses. Children who are not diagnosed early enough in life can develop amblyopia (lazy eye), which can be irreversible. Angle-closure glaucoma results from obstruction of the eye's outflow channels (trabecular meshwork) by the iris, which can produce increased intraocular pressure and subsequent damage to the optic nerve. The strong association of angle-closure glaucoma with nanophthalmos is thought to result from the ocular anatomical abnormalities seen in this condition (Brockhurst 1974; Kimbrough et al. 1979). Although medical treatment and laser surgery can be used to successfully manage angle-closure glaucoma in the nanophthalmic eye, untreated angle-closure glaucoma can result in blindness. In addition, complications following any type of intraocular surgery in the nanophthalmic eye are common and can cause severe loss of vision (Singh et al. 1982).

We began our investigation of the genetic causes of nanophthalmos with a molecular-genetic study of a single large kindred noted to have an unusually high incidence of high hyperopia and frequent occurrence of angle-closure glaucoma. As a first step toward identification of the disease gene and the underlying causes

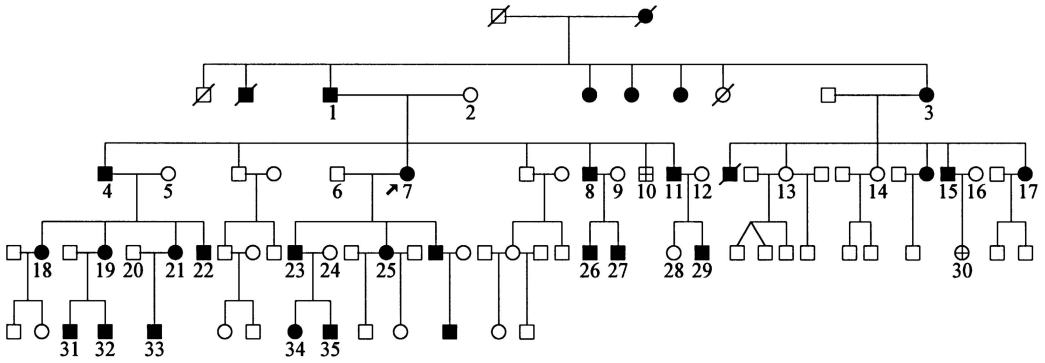

Figure 1 Nanophthalmos pedigree UM:181. Squares indicate males, and circles indicate females. Subjects with nanophthalmos are indicated by blackened symbols, those with intermediate phenotypes are indicated by cross-hatched symbols, and those with no known eye disease are indicated by unblackened symbols. The proband is indicated by an arrow. Deceased individuals are indicated by a diagonal line through the symbol. Numbered individuals were examined by the authors, as described in Subjects and Methods. Genotypes for individuals 1–15, 17–19, 21, 22, 24–27, 29, 31, 32, 34, and 35 were used in the analyses. This family is part of a much larger family from which recruitment is continuing.

of aberrant eye development in this family, we characterized the ocular features of each family member participating in the study, evaluated the mode of inheritance, and conducted a genome scan to search for genetic markers that cosegregate with the disease phenotype. Linkage and haplotype analyses of the resulting phenotypic and genotypic data provided strong evidence that a locus on chromosome 11 is responsible for autosomal dominant nanophthalmos in this family.

Subjects and Methods

Subjects

Thirty-five individuals in family UM:181 (fig. 1) were evaluated by ophthalmologic examination by three of the authors (D.A.C., G.L.S., and S.A.S.). Family members examined included 27 at-risk descendants of the affected founder and 8 unaffected spouses of affected family members. Complete ophthalmologic examination included refraction (reported as the spherical equivalent, in diopters), keratometry, slit-lamp biomicrosopy, gonioscopy, measurement of intraocular pressure, optic-disc evaluation, and A-scan ultrasonography to determine axial length. The ages of the affected individuals included in the genotyping and the analysis were within the range 7–77 years (mean 28.3 years).

Genotyping

Genomic DNA isolated by use of the Puregene kit (Gentra Systems), from 3-ml aliquots of whole blood, was diluted to a concentration of 50 ng/μl. AmpliTaq gold was used, in accordance with the manufacturer's recommended protocols (Perkin Elmer), to perform PCR amplifications in 15-μl reaction mixtures (Mullis and Faloona 1987). The microsatellite repeat markers assayed included 345 markers from the 22 autosomes (ABI Prism Linkage Mapping Panels). One of each pair of primers was labeled with phosphoramidite fluorescent tags, for use on an ABI377 semiautomated sequencer. Thermal cycling in a GeneAmp 9600 or a GeneAmp 9700 (Perkin Elmer) thermal cycler was performed at 95°C for 10–12 min, followed by 10 cycles at 94°C for 15 s, 55°C for 15 s, and 72°C for 30 s and 20 cycles at 89°C for 15 s, 55°C for 15 s, and 72°C for 30 s, followed by a 10–30 min extension at 72°C and a hold at 4°C. For the genome scan, multiplex loading of fragments with different dye labels that migrate in different size bins allowed simultaneous scoring of up to 14 fragments per lane. The resulting PCR products were denatured, size fractionated, and analyzed on 4% denaturing acrylamide run on an ABI377 semiautomated sequencer. GS350 or GS500 size standards were used as internal standards that were run in the same lane with the markers. Alleles read and scored by use of GeneScan and Genotyper software (ABI Perkin Elmer) were confirmed by eye. Analysis of 132 markers was completed before we identified linkage to the chromosome 11 markers. After the genome scan, some additional markers (Dib et al. 1996; Généthon; Genome Database) were assayed by radioactive labeling and autoradiography, as described elsewhere (Richards et al. 1994), to further reduce the chromosome 11 genetic inclusion interval (D11S1776, D11S903, D11S1313, and D11S4191) and to exclude the congenital microphthalmia locus on chromosome 14 (D14S977 and D14S1054). Amplification was performed in 10-μl reaction volumes, for 30–35 cycles, by use of the thermal-cycling conditions described by Morissette et al. (1995).

Statistical Methods

Two-point linkage analysis was performed with the MENDEL program (Lange et al. 1988), in accordance

Table 1

Two-Point LOD Scores for Linkage between Nanophthalmos and Chromosome 11 Markers in Family UM:181

	LOD Score at θ =									
Marker	.00	.01	.05	.10	.20	.30	.40	$\hat{\theta}$	$\hat{Z}$	$\theta(-2)$
D11S1338	$-\infty$	−5.00	−1.76	−.57	.27	.45	.32	.30	.45	.04
D11S902	$-\infty$	−4.51	−1.28	−.13	.64	.72	.48	.27	.74	.03
D11S904	$-\infty$	−3.76	−1.16	−.20	.45	.55	.38	.28	.56	.02
D11S1776	$-\infty$	3.20	3.56	3.43	2.81	1.96	.97	.05	3.56	.00
D11S935	$-\infty$	−.23	.36	.53	.56	.45	.26	.16	.58	.00
D11S905	$-\infty$	3.51	3.86	3.71	3.04	2.14	1.05	.05	3.86	.00
D11S903	5.92	5.83	5.44	4.94	3.85	2.65	1.31	.00	5.92	.00
D11S1313	4.10	4.03	3.75	3.39	2.62	1.77	.83	.00	4.10	.00
D11S4191	4.60	4.54	4.26	3.88	3.04	2.07	1.00	.00	4.60	.00
D11S987	$-\infty$	2.39	2.81	2.74	2.26	1.57	.74	.06	2.81	.00
D11S1314	$-\infty$	.62	2.22	2.64	2.51	1.88	.96	.13	2.68	.00
D11S937	$-\infty$	−.13	1.52	2.00	2.01	1.53	.78	.15	2.09	.00
D11S901	$-\infty$	−1.07	.64	1.19	1.37	1.10	.60	.18	1.38	.00
D11S1358	$-\infty$	−2.48	−.08	.75	1.18	1.02	.58	.21	1.18	.01
D11S898	$-\infty$	−4.31	−1.65	−.62	.15	.32	.20	.30	.32	.04
D11S908	$-\infty$	−5.98	−2.67	−1.41	−.42	−.09	−.02	.50	.00	.07

Note.—Linkage analyses were performed under the assumption of an autosomal dominant mode of inheritance with complete penetrance and a disease-allele frequency of .01.

with the LOD-score method (Morton 1955). Multipoint likelihoods were calculated with the VITESSE program (O'Connell and Weeks 1995). Allele frequencies were estimated from family data, as described elsewhere (Boehnke 1991). Linkage analyses were performed under a model of autosomal dominant inheritance with complete penetrance and a disease-allele frequency of .01. In tables 1–3, the column "$\theta(-2)$" indicates the largest recombination fraction (θ) at which linkage may be excluded on the basis of a LOD score <-2.00. $\hat{\theta}$ is the recombination fraction at which the estimated maximum LOD score $\hat{Z}$ is observed.

For the linkage study, the criteria for assignment of affected status included axial length <20.00 mm and refractive error >+7.00 diopters. For the genome scan, angle-closure glaucoma or occludable anterior-chamber angles were not part of the criteria for assignment of affected status. Individuals were considered unaffected if they had axial length >21.00 mm, refractive error <+4.00 diopters, and no evidence of angle-closure glau-

Table 2

Two-Point LOD Scores for Linkage between Angle-Closure Glaucoma and Chromosome 11 Markers in Family UM:181

	LOD Score at θ =									
Marker	.00	.01	.05	.10	.20	.30	.40	$\hat{\theta}$	$\hat{Z}$	$\theta(-2)$
D11S1338	$-\infty$	−6.52	−3.16	−1.83	−.68	−.19	.00	.45	.02	.09
D11S902	$-\infty$	−6.36	−3.04	−1.70	−.56	−.09	.07	.42	.07	.08
D11S904	$-\infty$	−4.54	−1.91	−.90	−.10	.17	.17	.35	.20	.04
D11S1776	$-\infty$	.63	1.15	1.23	1.05	.71	.33	.09	1.23	.00
D11S935	−.32	−.30	−.26	−.22	−.16	−.10	−.05	.50	.00	.00
D11S905	$-\infty$	1.43	1.91	1.93	1.61	1.12	.52	.08	1.94	.00
D11S903	3.21	3.16	2.93	2.64	2.02	1.34	.63	.00	3.21	.00
D11S1313	1.69	1.66	1.52	1.35	.99	.60	.23	.00	1.69	.00
D11S4191	3.09	3.04	2.82	2.54	1.94	1.29	.60	.00	3.09	.00
D11S987	2.05	2.01	1.85	1.65	1.23	.77	.30	.00	2.05	.00
D11S1314	$-\infty$	−.05	.99	1.29	1.28	.94	.46	.14	1.34	.00
D11S937	$-\infty$	−.29	.78	1.10	1.13	.85	.41	.15	1.17	.00
D11S901	$-\infty$	−1.16	−.04	.36	.55	.47	.26	.20	.55	.00
D11S1358	$-\infty$	−.86	.24	.62	.76	.62	.34	.18	.76	.00
D11S898	$-\infty$	−1.63	−.35	.08	.32	.27	.12	.22	.32	.00
D11S908	$-\infty$	−4.99	−2.34	−1.32	−.50	−.20	−.09	.50	.00	.06

Note.—Linkage analyses were performed under the assumption of an autosomal dominant mode of inheritance with complete penetrance and a disease-allele frequency of .01.

Table 3

Two-Point LOD Scores for Linkage between Nanophthalmos and Chromosome 14 Markers in Family UM:181

	LOD Score at θ =									
Marker	.00	.01	.05	.10	.20	.30	.40	$\hat{\theta}$	$\hat{Z}$	$\theta(-2)$
D14S261	$-\infty$	−5.69	−2.50	−1.23	−.21	.14	.18	.36	.19	.06
D14S70	$-\infty$	−19.48	−10.57	−6.88	−3.44	−1.67	−.61	.50	.00	.27
D14S276	$-\infty$	−11.42	−5.94	−3.69	−1.64	−.66	−.16	.50	.00	.17
D14S63	$-\infty$	−5.95	−2.64	−1.38	−.37	.00	.09	.40	.09	.07
D14S258	$-\infty$	−11.80	−5.76	−3.36	−1.31	−.43	−.05	.47	.01	.15
D14S74	$-\infty$	−4.33	−1.92	−1.03	−.33	−.05	.04	.41	.04	.04
D14S68	$-\infty$	−4.67	−2.02	−.99	−.17	.11	.14	.36	.15	.05
D14S280	$-\infty$	−1.48	−.77	−.43	−.07	.09	.11	.36	.12	.00
D14S977	$-\infty$	−8.37	−3.87	−2.11	−.65	−.06	.12	.41	.12	.10
D14S1054	$-\infty$	−7.24	−3.37	−1.84	−.59	−.12	.02	.43	.02	.09
D14S65	$-\infty$	−3.11	−1.20	−.43	.13	.24	.17	.30	.24	.02
D14S78	$-\infty$	−8.85	−4.17	−2.33	−.78	−.16	.06	.43	.06	.11
D14S292	$-\infty$	−11.11	−5.69	−3.51	−1.57	−.66	−.20	.50	.00	.16

Note.—Linkage analysis excluded the *CMIC* locus in the 12.6-cM D14S977–D14S1054–D14S65 interval.

coma or occludable anterior-chamber angles. Individuals of intermediate phenotype were scored as undesignated. Once linkage to chromosome 11 markers was detected, two-point linkage analysis was repeated by use of a more stringent phenotype in which only individuals with angle-closure glaucoma or occludable anterior-chamber angles were considered to be affected. The results of both analyses for the chromosome 11 markers are shown in tables 1 and 2. Flanking markers identified by linkage analysis were confirmed by haplotype analysis (fig. 3).

Results

In family UM:181, nanophthalmos is inherited in an autosomal dominant manner (fig. 1). Objective measures of axial length (measured from front to back of the eye) and refraction (amount of optical correction required for best achievable vision) readily distinguish affected individuals from unaffected individuals. Affected family members demonstrated high hyperopia, within the range +7.25–+13.00 diopters (mean +9.88 diopters). In comparison, the emmetropic (normal) eye has a refraction of −1.00–+1.00 diopters. In general, someone with a refraction outside of this range will require corrective lenses for some or all of their daily visual tasks. In affected family members, the mean axial length was reduced to 18.13 mm (range 17.55–19.28 mm), which is <80% of the mean axial length of 23.37 mm in the normal individuals described by Francois and Goes (1977). Angle-closure glaucoma or occludable anterior-chamber angles, present in 12 of the 22 affected individuals, represent later stages of progression of the phenotype but are not necessary to identify affected individuals. Eleven unaffected subjects in the study had open angles, refraction of −1.38–+3.38 diopters, and axial length of 21.26–24.48 mm. Two borderline subjects were not included in the linkage study.

Two-point linkage analysis provided strong evidence for linkage of the nanophthalmos phenotype to marker D11S903 ($\hat{Z} = 5.92$ at $\hat{\theta} = .00$) and four other nearby markers (table 1). Multipoint analysis revealed a maximum LOD score of 6.31 at D11S1313 (fig. 2). Both linkage analysis and haplotyping indicate that this locus, called *"NNO1"* (Genome Database Nomenclature Committee), is located within a 14.7-cM genetic inclusion interval framed by recombination events at D11S905 and D11S987. The distal boundary of the interval was defined by a recombination event between D11S4191 and D11S987 that was observed in individual 35 (fig. 3). Similarly, the proximal boundary of the interval is based on a recombination event between D11S905 and D11S903 that was detected on the chromosome that individual 35 inherited from individual 23 (fig. 3). When the phenotype was limited to angle-closure glaucoma and/or occludable angles, the level of significance of the linkage observation was reduced but still significant, with LOD scores >3.0 for two of the markers ($\hat{Z} = 3.21$ at $\hat{\theta} = .00$ for D11S903, and $\hat{Z} = 3.09$ at $\hat{\theta} = .00$ for D11S4191; table 2). Our linkage results exclude the autosomal recessive congenital microphthalmia locus (*CMIC;* MIM 251600), which has been localized between D14S987 and D14S267 on chromosome 14q32 (Bessant et al. 1998; table 3).

Since nanophthalmos can be scored based solely on the basis of objective characteristics that are evident even in very young family members, we were able to recruit a large number of affected participants who would have been excluded from a study aimed at mapping the angle-closure–glaucoma phenotype. Thus, although angle-clo-

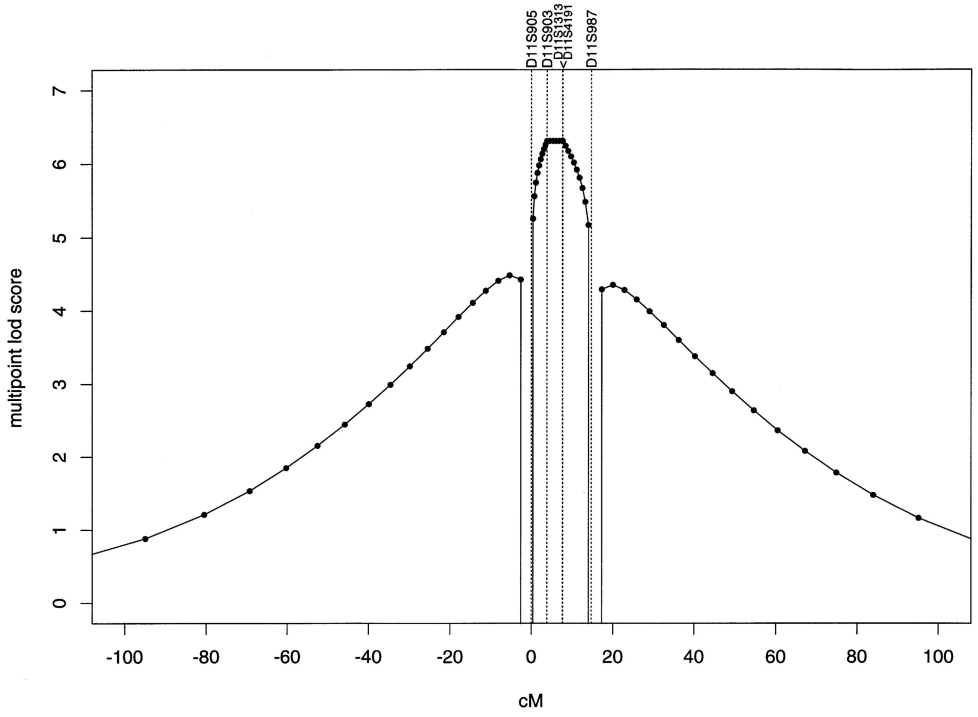

Figure 2 Multipoint analysis of markers immediately around the *NNO1* locus. Dots represent locations for which multipoint LOD scores were calculated, to determine linkage between nanophthalmos and the marker map D11S905–3.8 cM–D11S903–3.8 cM–D11S1313–0.1 cM–D11S4191–7.0 cM–D11S987. Dotted lines indicate the positions of these markers. Only one dotted line is shown for D11S1313 and D11S4191, because they are so close together. LOD scores of $-\infty$ at D11S905 and D11S987 are not shown.

sure glaucoma is a potentially serious consequence of nanophthalmos, for many family members, the age-dependent penetrance of glaucoma would have caused loss of useful information if angle-closure glaucoma had been the primary trait scored for the genome scan.

Discussion

Linkage analysis of data from the genome scan provided very strong evidence that a genetic defect on chromosome 11, between D11S905 and D11S987, is responsible for autosomal dominant nanophthalmos in family UM:181. The genome scan that mapped this *NNO1* locus was performed by use of the limited set of objective measures of nanophthalmos as the basis for assignment of affected status. We also found significant evidence that markers from this region of 11p are linked to the more severe late-stage phenotype of angle-closure glaucoma/occludable anterior-chamber angles found in this family. The mapping of both traits, nanophthalmos and angle-closure glaucoma, to the same locus is consistent with previous reports that angle-closure glaucoma is highly associated with nanophthalmos (Brockhurst 1974; Kimbrough et al. 1979).

The *NNO1* defect produces a set of ocular characteristics that include high hyperopia, short axial length, and predisposition to angle-closure glaucoma, in family UM:181. Most affected family members began wearing glasses at preschool age, sometimes as early as 1 year of age, and some family members appear to have amblyopia. More than half of the affected family members have been diagnosed with angle-closure glaucoma or anterior-chamber angles that are narrow enough to be in danger of angle closure. A substantial number of the affected individuals in the first and second generations of family UM:181 have suffered significant visual loss from angle-closure glaucoma and complications of ocular surgery. Some younger family members have already undergone laser surgery. Even with intervention and careful monitoring, they are still at risk for progressive glaucomatous damage and visual loss.

The clinical characteristics, mode of inheritance, and map location indicate that the *NNO1* locus is distinct from the congenital microphthalmia locus on 14q32 (MIM 251600; Bessant et al. 1998), the locus for Lenz microphthalmia (MIM 309800; Lenz 1955; Ogunye et al. 1975), and that for oculodentodigital syndrome (MIM 164200; Rajic and De Veber 1966; Gladwin et al. 1997). Clinical features and mode of inheritance suggest that UM:181 nanophthalmos is a different pheno-

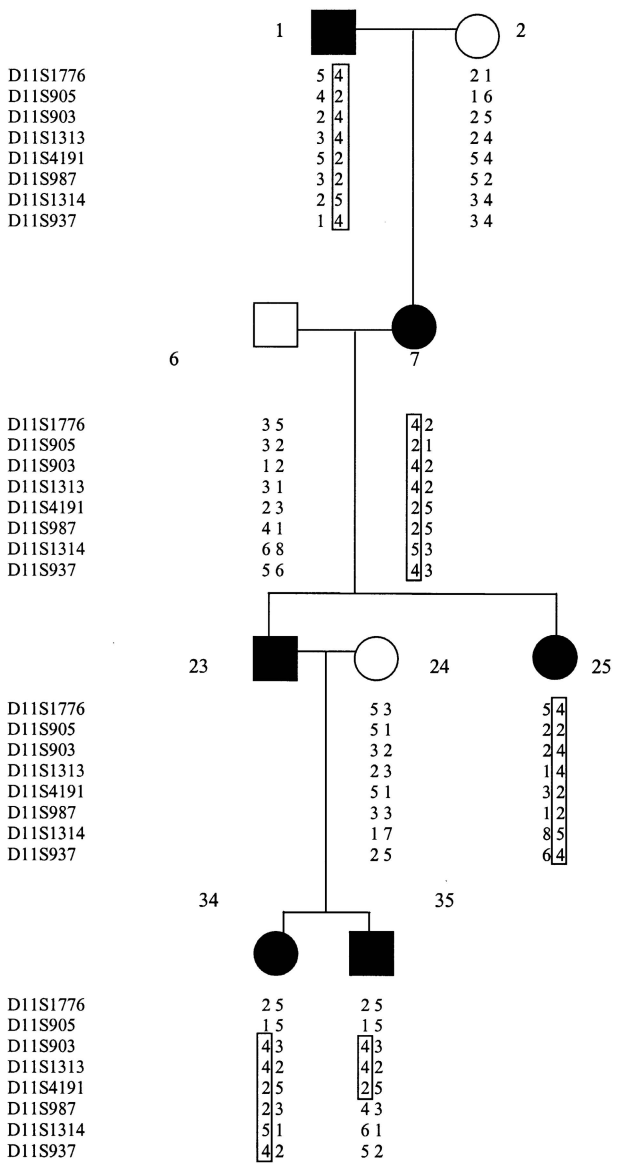

Figure 3 Haplotype analysis. Squares indicate males, and circles indicate females. The individual numbers correspond to the individual numbers in the pedigree in fig. 1. Subjects with nanophthalmos are indicated by blackened symbols, and those with no known eye disease are indicated by unblackened symbols. Alleles of the disease gene–bearing haplotype are contained within the boxed portions of the haplotypes. At the time these markers were run, DNA was not available from individual 23, the father of individuals 34 and 35.

type, rather than a form of retinal degeneration with nanophthalmos, cystic macular degeneration, and angle-closure glaucoma (MIM 267760), described by MacKay and colleagues (1987). Because the glaucoma in nanophthalmos results from an angle-closure mechanism, it is not surprising that our data also exclude the reported primary open-angle glaucoma loci *GLC1A* (MIM 137750; Sheffield et al. 1993), *GLC1B* (MIM 137760; Stoilova et al. 1996), *GLC1C* (MIM 601682; Wirtz et al. 1997), and *GLC1D* (MIM 602429; Trifan et al., 1998). Testing of other nanophthalmos families, with markers in the immediate vicinity of the *NNO1* locus, will allow us to test for genetic heterogeneity for nanophthalmos. Testing of other families with related but different phenotypes will allow us to determine whether less severe forms of hyperopia or other forms of angle-closure glaucoma might also map to this locus.

Nanophthalmos is thought to result from the arrested development of the eye during the embryonic stage (Duke-Elder 1964), but the specific underlying genetic and biochemical causes are unknown. Studies of animal models and hereditary human ocular disorders indicate that multiple transcriptional activators play important roles in eye development in animal model systems, but the factors that determine globe size in humans are not well understood (Jordan et al. 1992; Burmeister et al. 1996; Sanyanusin et al. 1995; Graw 1996; Belecky-Adams et al. 1997; Furukawa et al. 1997; Freund et al. 1998). Thickened sclera is a common manifestation of nanophthalmos, and some studies have reported unusual collagen bundles and aberrant glycosaminoglycan metabolism in some, but not all, cases (Yue et al. 1988; David et al. 1990; Shiono et al. 1992). However, the relationship of these aberrant structural and metabolic properties to the causes of human nanophthalmos remains poorly defined.

Owing to the apparently developmental nature of the *NNO1* defect, we were interested to find that one of the genes located on 11 is the *PAX6* gene (MIM 106210), a homeodomain gene that produces a protein known to play a critical role in ocular development in mice and humans (Graw 1996; Tomarev 1997; Tang et al. 1998). The mouse *Pax6* gene has been implicated in the phenotype "small eye" in mice, but reduced globe size is not a feature of aniridia (MIM 106210; Mouse Genome Informatics) or of the several other ocular phenotypes reported for *PAX6* defects in humans (MIM 106210; Jordan et al. 1992; Glaser et al. 1994*a;* Hanson et al. 1994; Mirzayans et al. 1995; Azuma et al. 1996; Schedl et al. 1996). In the Unigene Human Sequence Collection database (National Center for Biotechnology Information), the *PAX6* UniGene cluster, Hs.89506, is located in the 38–42-cM region of chromosome 11 between markers D11S1324 and D11S914. The proximal marker for this bin, D11S914, is 12 cM telomeric to D11S905, the distal flanking marker for the *NNO1* interval (Dib et al. 1996). Glaser and colleagues (1994*b*) used somatic-cell hybrids containing deletions in human chromosome 11 to place *PAX6* distal to D11S907, which is 8.1 cM distal to D11S905 (Dib et al. 1996). Thus, a defect in *PAX6* appears to be ruled out as the cause of nanophthalmos in family UM:181, on the basis of the placement of *PAX6* outside of the *NNO1* genetic inclusion

interval. We are continuing our evaluation of additional genes in the region as potential *NNO1* candidates, including more precise localization of genes for which previous placements are approximate.

The mapping of the *NNO1* locus is the first step toward the identification of the gene itself. When the gene is known, genetic testing of at-risk individuals will be possible, allowing early detection and treatment. Such testing may be particularly beneficial with respect to early treatment of children with hyperopia, to prevent amblyopia. Testing also would identify individuals in need of long-term follow-up to monitor for development of angle-closure glaucoma. In addition to providing information about the first genetically mapped form of autosomal dominant nanophthalmos, identification of the *NNO1* gene should provide further insights into fundamental aspects of ocular development.

Acknowledgments

This study was supported, in part, by National Institutes of Health grants EY09580 and EY11671 (to J.E.R.), EY114405 (to D.V.), and EY07003 (University of Michigan–Core); National Center for Research Resources grant M01 RR 00042 (University of Michigan–General Clinical Research Center); the Glaucoma Research Foundation; the Helen Van Arnam Glaucoma Research Fund of the University of Michigan; and unrestricted grants to the Dean A. McGee Eye Institute and to the W. K. Kellogg Eye Center, from Research to Prevent Blindness.

Electronic-Database Information

Accession numbers and URLs for data in this article are as follows:

ABI Prism Linkage Mapping Panels, http://www.CHLC.org/ABI/ABIRefMaps.html (for genetic markers used in the genome scan)

Généthon, http://www.genethon.fr (for information on genetic markers used in the genome scan and in subsequent refinement of the genetic inclusion interval)

Genome Database, http://gdbwww.gdb.org (for assignment of gene and locus names)

Genome Database Nomenclature Committee, http://www.gene.ucl.ac.uk/nomenclature/ (for assignment of gene and locus names)

Mouse Genome Informatics, The Jackson Laboratory, http://www.informatics.jax.org/mrktools.html (for information on mouse *Sey* ["small eye"] and ocular retardation mutants)

National Center for Biotechnology Information, http://www.ncbi.nlm.nih.gov/ (for information on *PAX6* [accession no. Hs89506] localization relative to *NNO1*)

Online Mendelian Inheritance in Man (OMIM), http://www.ncbi.nlm.nih.gov/Omim (for congenital microphthalmia [MIM 251600]; Lenz microphthalmia [MIM 309800]; oculodentodigital syndrome [MIM 164200]; retinal degeneration with nanophthalmos, cystic macular degeneration, and angle-closure glaucoma [MIM 267760]; aniridia [MIM 106210]; isolated foveal hypoplasia [MIM 106210]; Leber congenital amaurosis [MIM 602225]; congenital cataracts, aniridia, anophthalmia, and CNS defects [MIM 106210]; *GLC1A* [MIM 137750]; *GLC1B* [MIM 137760]; *GLC1C* [MIM 601682]; *GLC1D* [MIM 602429]; and *PAX6* [MIM 106210])

Unigene Human Sequence Collection, National Center for Biotechnology Information, http://www.ncbi.nlm.nih.gov/UniGene/Hs.Home.html (for information on *PAX6* [accession no. Hs.89506] localization relative to *NNO1*)

References

Azuma N, Nishina S, Yanagisawa H, Okuyama T, Yamada M (1996) *PAX6* missense mutation in isolated foveal hypoplasia. Nat Genet 13:141–142

Belecky-Adams T, Tomarev S, Li HS, Ploder L, McInnes RR, Sundin O, Adler R (1997) Pax-6, Prox 1, and Chx10 homeobox gene expression correlates with phenotypic fate of retinal precursor cells. Invest Ophthalmol Vis Sci 38: 1293–1303

Bessant DAR, Khaliq S, Hameed A, Anwar K, Mehdi SQ, Payne AM, Battacharya SS (1998) A locus for autosomal recessive congenital microphthalmia maps to chromosome 14q32. Am J Hum Genet 62:1113–1116

Boehnke M (1991) Allele frequency estimation from data on relatives. Am J Hum Genet 48:22–25

Brockhurst RJ (1974) Nanophthalmos with uveal effusion: a new clinical entity. Trans Am Ophthalmol Soc 72:371–403

Burmeister M, Novak J, Liang MY, Basu S, Ploder L, Hawes NL, Vigden D, et al (1996) Ocular retardation mouse caused by Chx10 homeobox null allele: impaired retinal progenitor proliferation and bipolar cell differentiation. Nat Genet 12: 376–384

David T, Chauvaud D, Pouliquen Y (1990) Nanophthalmos with uveal effusion. Bull Soc Ophtalmol Fr 90:263–265

Dib C, Fauré S, Fizames C, Samson D, Drouot N, Vignal A, Millasseau P, et al (1996) A comprehensive genetic map of the human genome based on 5,264 microsatellites. Nature 380:152–154

Diehl DL, Feldman F, Tanzer H, Shea M (1989) Nanophthalmos in sisters, one with exfoliation syndrome. Can J Ophthalmol 24:327–330

Duke-Elder S (1964) Anomalies in the size of the eye. In: Duke-Elder S (ed) System of ophthalmology. Vol 3, pt 2. CV Mosby, St Louis, pp 488–495

Francois J, Goes F (1977) Ultrasonographic study of 100 emmetropic eyes. Ophthalmologica 175:321–327

Freund CL, Wang QL, Chen S, Muskat BL, Wiles CD, Sheffield VC, Jacobson SG, et al (1998) De novo mutations in the CRX homeobox gene associated with Leber congenital amaurosis. Nat Genet 18:311–312

Furukawa T, Morrow EM, Cepko CL (1997) Crx, a novel otx-like homeobox gene, shows photoreceptor-specific expression and regulates photoreceptor differentiation. Cell 91: 531–541

Gladwin A, Donnai D, Metcalfe K, Schrander-Stumpel C, Brueton L, Verloes A, Aylsworth A, et al (1997) Localization

of a gene for oculodentodigital syndrome to human chromosome 6q22-q24. Hum Mol Genet 6:123–127

Glaser T, Jepeal L, Edwards JG, Young SR, Favor J, Maas RL (1994*a*) *PAX6* gene dosage effect in a family with congenital cataracts, aniridia, anophthalmia and central nervous system defects. Nat Genet 7:463–471

Glaser T, Ton CCT, Mueller R, Petzl-Erler ML, Oliver C, Nevin NC, Housman DE, et al (1994*b*) Absence of PAX6 gene mutations in Gillespie syndrome (partial aniridia, cerebellar ataxia, and mental retardation). Genomics 19:145–148

Graw J (1996) Genetic aspects of embryonic eye development in vertebrates. Dev Genet 18:181–197

Hanson IM, Fletcher JM, Jordon T, Brown A, Taylor D, Adams RJ, Punnett HH, et al (1994) Mutations at the *PAX6* locus are found in heterogeneous anterior segment malformations including Peters' anomaly. Nat Genet 6:168–173

Jordan T, Hanson I, Zaletayev D, Hodgson S, Prosser J, Seawright A, Hastie N, et al (1992) The human *PAX6* gene is mutated in two patients with aniridia. Nat Genet 1:328–332

Kimbrough RL, Trempe CS, Brockhurst RJ, Simmons RJ (1979) Angle-closure glaucoma in nanophthalmos. Am J Ophthalmol 88:572–579

Lange K, Weeks D, Boehnke M (1988) Programs for pedigree analysis: MENDEL, FISHER, and dGENE. Genet Epidemiol 5:471–472

Lenz W (1955) Recessiv-geschlechtsgebundene Mikrophthalmie mit multiplen Missbildungen. Z Kinderheilk 77: 384–390

MacKay CJ, Shek MS, Carr RE, Yanuzzi LA, Gouras P (1987) Retinal degeneration with nanophthalmos, cystic macular degeneration, and angle-closure glaucoma: a new recessive syndrome. Arch Ophthalmol 105:366–371

Martorina M (1988) Familial nanophthalmos. J Fr Ophtalmol 11:357–361

Mirzayans F, Pearce WG, MacDonald IM, Walter MA (1995) Mutation of the *PAX6* gene in patients with autosomal dominant keratitis. Am J Hum Genet 57:539–548

Morissette J, Cote G, Anctil JL, Plante M, Amyot M, Heon E, Trope GE, et al (1995) A common gene for juvenile and adult-onset primary open-angle glaucomas confined on chromosome 1q. Am J Hum Genet 56:1431–1442

Morton NE (1955) Sequential tests for the detection of linkage. Am J Hum Genet 7:277–318

Mullis KB, Faloona FA (1987) Specific synthesis of DNA in vitro via a polymerase chain reaction. Methods Enzymol 155:335–350

O'Connell JR, Weeks DE (1995) The VITESSE algorithm for rapid exact multilocus linkage analysis via genotype set-recoding and fuzzy inheritance. Nat Genet 11:402–408

Ogunye OO, Murray RF Jr, Osgood T (1975) Linkage studies in Lenz microphthalmia. Hum Hered 25:493–500

Rajic DS, De Veber LL (1966) Hereditary oculodentoosseous dysplasia. Ann Radiol 9:224–231

Richards JE, Lichter PR, Boehnke M, Uro JL, Torrez D, Wong D, Johnson AT (1994) Mapping of a gene for autosomal dominant juvenile-onset open-angle glaucoma to chromosome 1q. Am J Hum Genet 54:62–70

Sanyanusin P, Schimmenti LA, McNoe LA, Ward TA, Pierpont ME, Sullivan MJ, Dobyns WB, et al (1995) Mutation of the PAX2 gene in a family with optic nerve colobomas, renal anomalies and vesicoureteral reflux. Nat Genet 9:358–364

Schedl A, Ross A, Lee M, Engelkamp D, Rashbass P, van Heyningen V, Hastie ND (1996) Influence of *PAX6* gene dosage on development: overexpression causes severe eye abnormalities. Cell 86:71–82

Sheffield VC, Stone EM, Alward WL, Drack AV, Johnson AT, Streb LM, Nichols BE (1993) Genetic linkage of familial open angle glaucoma to chromosome 1q21-q31. Nat Genet 4:47–50

Shiono T, Shoji A, Mutoh T, Tamai M (1992) Abnormal sclerocytes in nanophthalmos. Graefes Arch Clin Exp Ophthalmol 230:348–351

Singh OS, Simmons RJ, Brockhurst RJ, Singh OS (1982) Nanophthalmos: a perspective on identification and therapy. Ophthalmology 89:1006–1012

Stoilova D, Child A, Trifan OC, Crick RP, Coakes RL, Sarfarazi M (1996) Localization of a locus (GLC1B) for adult-onset primary open angle glaucoma to the 2cen-q13 region. Genomics 36:142–150

Tang HK, Singh S, Saunders GF (1998) Dissection of the transactivation function of the transcription factor encoded by the eye developmental gene *PAX6*. J Biol Chem 273: 7210–7221

Tomarev SI (1997) Pax-6, eyes absent, and Prox 1 in eye development. Int J Dev Biol 41:835–842

Trifan OC, Traboulsi EI, Stoilova D, Alozie I, Nguyen R, Raja S, Sarfarazi M (1998) The third locus (GLC1D) for adult-onset primary open-angle glaucoma maps to the 8q23 region. Am J Ophthalmol 126:17–28

Vingolo EM, Steindl K, Forte R, Zompatori L, Iannaccone A, Sciara A, Del Porto G, et al (1994) Autosomal dominant simple microphthalmos. J Med Genet 31:721–725

Weiss AH, Kousseff BG, Ross EA, Longbottom J (1989) Simple microphthalmos. Arch Ophthalmol 107:1625–1630

Wirtz MK, Samples JR, Kramer PL, Rust K, Topinka JR, Yount J, Koler RD, et al (1997) Mapping a gene for adult-onset primary open angle glaucoma to chromosome 3q. Am J Hum Genet 60:296–304

Yue BY, Kurosawa A, Duvall J, Goldberg MF, Tso MO, Sugar J (1988) Nanophthalmic sclera: fibronectin studies. Ophthalmology 95:56–60